Voltage-Dependence of Virus-encoded Miniature K+ Channel Kcv

ARTICLE *in* JOURNAL OF MEMBRANE BIOLOGY · JUNE 2002

Impact Factor: 2.46 · DOI: 10.1007/s00232-001-0147-5 · Source: PubMed

5 AUTHORS, INCLUDING:

Sabrina Gazzarrini
University of Milan
28 PUBLICATIONS **631** CITATIONS

SEE PROFILE

Anna Moroni
University of Milan
110 PUBLICATIONS **1,948** CITATIONS

SEE PROFILE

J. Membrane Biol. 187, 15–25 (2002)
DOI: 10.1007/s00232-001-0147-5

The Journal of
Membrane
Biology

Voltage-Dependence of Virus-encoded Miniature K^+ Channel Kcv

S. Gazzarrini[1], J.L. Van Etten[2], D. DiFrancesco[3], G. Thiel[4], A. Moroni[1]
[1]Department of Biology, CNR-Centro per la Biologia Molecolare e Cellulare delle Piante-Università degli Studi di Milano, via Celoria 26, 20133 Milano, Italy
[2]Department of Plant Pathology, University of Nebraska, Lincoln, NE 8583-0722, USA
[3]Department of General Physiology and Biochemistry, Università degli Studi di Milano, Italy
[4]Institute for Botany, University of Technology, Darmstadt, Germany

Received: 12 July 2001/Revised: 28 January 2002

Abstract. Kcv is a K^+-selective channel encoded by the *Paramecium bursaria Chlorella* virus 1 (PBVC-1). Expression of this protein, so far the smallest known functional K^+ channel, in *Xenopus* oocytes reveals an instantaneous and a time-dependent component during voltage-clamp steps. These two components have an identical sensitivity to the inhibitor amantadine, implying that they reflect distinct kinetic features of the same channel. About 70% of the channels are always open; at hyperpolarizing voltages the time-dependent channels (30%) open in a voltage-dependent manner reaching half-maximal activation at about −70 mV. At both extreme positive and negative voltages the open-channel conductance decreases in a voltage-dependent manner. To examine the mechanism underlying the voltage-dependence of Kcv we neutralized the two charged amino acids in the lipophilic N-terminus. However, this double mutation had no effect on the voltage-dependence of the channel, ruling against the possibility that these charged amino acids represent a membrane-embedded voltage sensor. We have considered whether a block by external divalent cations is involved in the voltage-dependence of the channel. The Kcv current was increased about 4-fold on reduction of external Ca^{2+} concentration by a factor of ten. This pronounced increase in current was observed on lowering Ca^{2+} but not Mg^{2+} and was voltage-independent. These data indicate a Ca^{2+}-selective, but voltage-independent mechanism for regulation of channel conductance.

Key words: K^+ channel — PBCV-1 — Kcv — Voltage-dependence — Ca^{2+} block

Correspondence to: A. Moroni; email: anna.moroni@unimi.it

Introduction

K^+ channels are tetramers of identical or similar subunits, arranged around a central ion-conducting pore. They are classified, according to their subunit transmembrane topology, into 6-, 4- and 2- transmembrane (TM)-domain channels. The smallest K^+ channels belong to the 2TM class and are formed by two TM domains connected by a stretch of amino acids (aa), the so-called pore (P) domain; this basic structure is also conserved in the pores of the more complex 4TM and 6TM channels (Wei et al., 1996; Clapham, 1999). Several 2TM K^+ channels have been cloned from animals and bacteria (Doupnik, Davidson & Lester, 1995; Schrempf et al., 1995). Among the class of 2TM channels, Kcv, the first K^+ channel cloned from a virus, is the smallest known to date (Plugge et al., 2000). It was discovered in the genome of PBCV-1 (*Paramecium bursaria Chlorella* virus), the prototype virus of the Phycodnaviridae family, which, to date, has about 50 members. PBCV-1 is a large icosahedral virus that infects and replicates in the single-cell green alga *Chlorella* strain NC64A (Van Etten & Meints, 1999). Kcv is a 94-aa long peptide. Hydropathy analysis reveals two putative TM domains separated by a stretch of 44 aa that contains the K^+ channel signature sequence THSTVGFG. The 26 aa surrounding this motif display, on average, 61% similarity and 38% identity with the pore domains of many K^+ channel proteins (Plugge et al., 2000).

The most remarkable structural feature of Kcv resides in the protein N- and C-termini. The cytoplasmic N-terminus is very short (12 aa) and contains two positively charged aa (K6, R10) and a putative casein kinase 2 (ck2) phosphorylation site (TRTE). In contrast to all other known K^+ channels, the protein lacks a cytoplasmic C-terminus (Plugge et al., 2000).

Kcv has been successfully expressed in a heterologous system (Plugge et al., 2000). In spite of its small size, it exhibits, when expressed in *Xenopus* oocytes, the typical features of a K^+ channel including ion selectivity, a moderate voltage-dependence and sensitivity to known channel blockers (Plugge et al., 2000). Since the structure of the Kcv pore resembles that of other known K^+ channels, information obtained from Kcv provides useful information on the basic principles of K^+ function. The understanding of ion permeation through K^+ channel pores and high-resolution structure-function relations currently are important topics in physiology and structural biology (Doyle et al., 1998; Perozo, Cortes & Cuello, 1998). Because of its small size, Kcv represents an interesting model system for studying many of the fundamental structure-function relations of K^+ channels.

Materials and Methods

The Kcv gene was cloned into pSGEM vector (a modified version of pGEM-HE, courtesy of M. Hollmann, Max Planck Institute for Experimental Medicine, Göttingen, Germany). The DNA templates were linearized with *Nsi*I and transcribed in vitro with T7 RNA polymerase. The mRNA was injected into *Xenopus laevis* oocytes, isolated according to standard methods (Moroni, Bardella & Thiel, 1998).

The mutant channel ΔN-Kcv was constructed by standard PCR techniques by deletion of the first 12 aa and inserted in pSGEM for oocyte expression. The fusion protein with GFP (ΔN-Kcv:GFP) was constructed by PCR amplification removing the stop codon from Kcv by means of a reversal PCR primer, subcloning the mutated ΔN-Kcv in frame and upstream of the GFP gene and moving the fusion protein (ΔN-Kcv:GFP) in pCDNA 3.1 (Invitrogen) for transfection in mammalian HEK 293 cells. Cell transfection was performed according to the calcium-phosphate method reported in Moroni et al., 2000.

Membrane current and voltage were recorded with a conventional two-electrode voltage-clamp method using the Gene Clamp 500 amplifier under control of pCLAMP 5.5 software (Axon Instruments, Foster City, CA). Electrodes were filled with 3 M KCl and had resistances between 0.4 and 1 MΩ in 50 mM KCl. The oocytes were perfused at room temperature (25–27°C) with a high-K^+ solution containing (mM): KCl 50, $CaCl_2$ 1.8, $MgCl_2$ 1, Hepes 5, pH 7.4 with KOH, at a rate of 2 ml min^{-1}. Mannitol was used to adjust the osmolarity to 215 mosmol. In some experiments the external Ca^{2+} concentration, $[Ca^{2+}]_o$, was reduced to 0.18 mM. Complete removal was not advisable since it caused activation of endogenous conductances.

Results

Kcv Generates a Conductance with two Kinetic Components

Xenopus oocytes injected with Kcv cRNA expressed a characteristic current (Fig. 1*A*) that was absent in H_2O-injected oocytes (Plugge et al., 2000). To differentiate the current through Kcv channels from the endogenous currents, an oocyte was treated with 6 mM amantadine. This inhibitor is an ideal tool to separate the Kcv current from the endogenous oocyte currents, because it has no effect on endogenous currents (*see* below), and blocks the Kcv-specific current in a voltage-independent manner (Plugge et al., 2000). The amantadine-sensitive current, shown in Fig. 1*C*, results from the subtraction of *B* from *A* and from now on will be referred to as Kcv current (I_{Kcv}).

To show that Kcv expresses a channel "per se" that is not due to an unspecific effect of Kcv-injection on endogenous oocytes conductances, we tested the ability of Kcv-mutants to generate currents in oocytes. Fig. 2 shows a representative example of the currents of an oocyte injected with a mutated channel (ΔN-Kcv), in which the N-terminus (aa 1–12) was deleted. These oocytes ($n = 15$) show essentially the same currents observed in H_2O-injected oocytes. Addition of 6 mM amantadine had only a minor effect on membrane currents (Fig. 2*B*,*C*), as observed in water-injected oocytes (*not shown*). The ΔN-Kcv channel was constructed also as a GFP fusion protein (ΔN-Kcv:GFP) and its expression pattern analyzed by confocal microscopy after transfection of mammalian HEK 293 cells. Its cellular distribution was identical to the wt Kcv:GFP-fusion protein. Furthermore, the wt-Kcv:GFP-fusion protein produced a transfection-specific current, whereas the ΔN-Kcv:GFP-fusion protein did not (*data not shown*). These results show that the mutant channel is synthesized but is unable to induce a change in conductance. Likewise, a point mutation in the selectivity filter region (F66A) of wt Kcv created a protein unable to generate currents above the endogenous current background in oocytes (Plugge et al., 2000). These experiments establish that the currents recorded in oocytes after injection with Kcv cRNA are, indeed, due to the expression of a K^+ channel and are not due to an unspecific upregulation of K^+ channels endogenous to the oocytes.

The Kcv steady-state current (I_{ss}, inset of Fig. 1) is plotted in the current/voltage relation shown in Fig. 1*D* (*open circles*) and appears to comprise two components, an instantaneous (I_i, inset of Fig. 1 and *closed circles* in Fig. 1*D*) and a time-dependent one (I_t, resulting from I_{ss}-I_i, inset of Fig. 1). These components display different sensitivities to voltage. Analysis of the current-voltage relations shows that I_i decreases at extreme positive and negative voltages, while I_t (I_{ss}-I_i) decreases at positive and increases at negative voltages.

The two different components of the Kcv-generated current shown in Fig. 1 could result either from two different channels or from two different kinetic properties of the same channel. To address this problem we investigated the effect of a lower (1 mM) concentration of amantadine on Kcv current. This

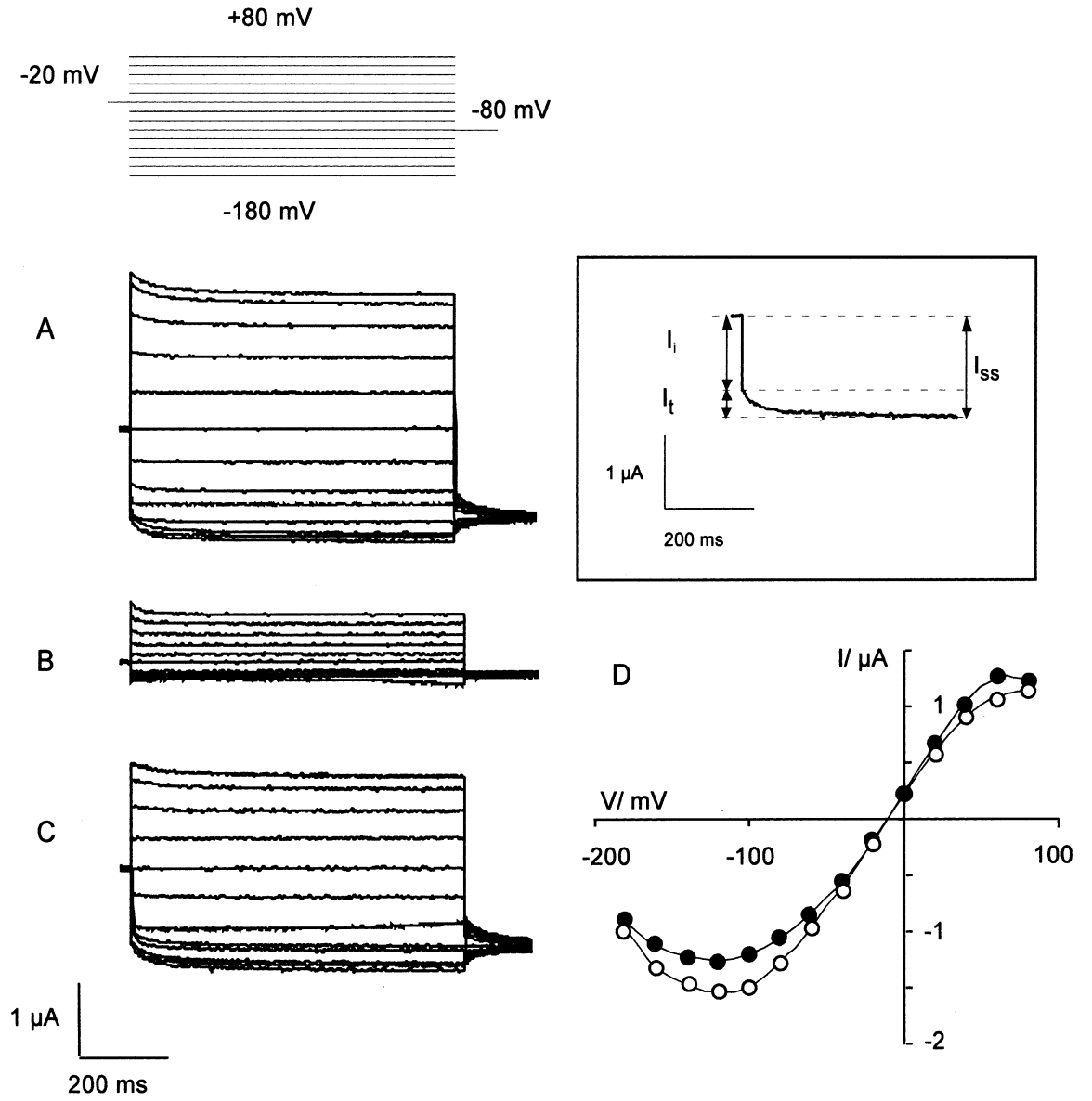

Fig. 1. Kcv currents in *Xenopus* oocytes. (*A*) Currents recorded in 50 mM KCl from one oocyte injected with Kcv mRNA were induced by voltage-steps from a holding potential (−20 mV) to test voltages as indicated. (*B*) Addition of 6 mM amantadine to the bath medium strongly reduced Kcv current leaving only oocyte endogenous current. (*C*) Subtraction of the currents (*A*−*B*) reveals the Kcv-specific current. (*D*) *I*/*V* relations from the data of C: (●) instantaneous and (○) steady-state current. *Inset:* exemplary separation of the steady-state current, I_{ss}, (recorded at −140 mV) into the instantaneous, I_i, and time-dependent, I_t, components.

concentration inhibits the Kcv current by 50% (Plugge et al., 2000) and hence allows one to measure the relative inhibition of I_i and I_t, respectively. The plots in Fig. 3*A* and *B* show that the instantaneous and the time-dependent currents were inhibited by amantadine in the same ratio and with the same voltage-dependence. Similar results were found in three more experiments. This supports the view that the Kcv current is due to the activity of one channel type with two different kinetic components. Since each of these two components has a distinct voltage-dependence, in the following we have proceeded to analyze the voltage-dependence of both kinetic components separately.

Instantaneous Component

To examine the voltage-dependent decrease of I_i at both negative and positive voltages we plotted the I_i/voltage relation from the experiment shown in Fig. 1 and extrapolated the linear portion between −20 mV and +20 mV on the assumption that this represents the maximal conductance of the I_i/V relation and thus the open-channel I/V relation (Fig. 4*A*). The

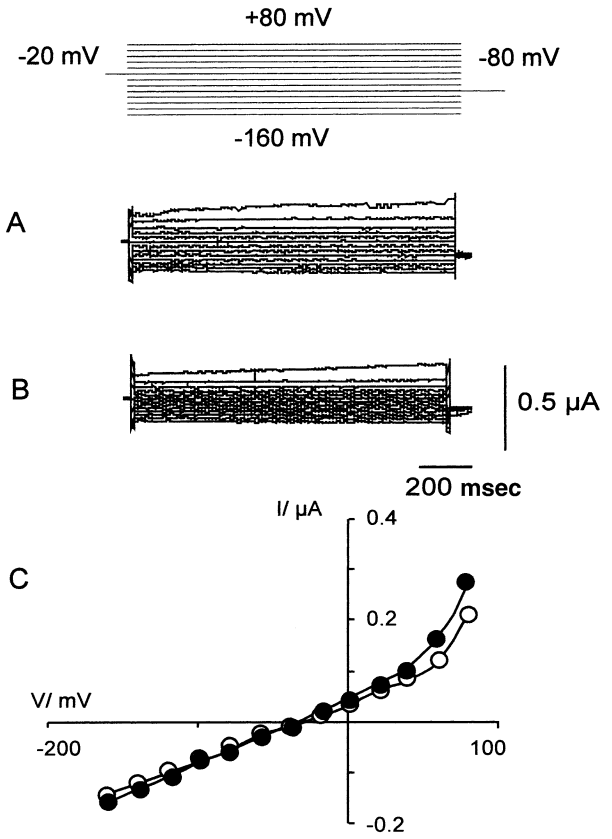

Fig. 2. Currents in *Xenopus* oocyte injected with the Kcv mutant ΔN-Kcv. (*A*) Currents recorded in 50 mM KCl from one oocyte injected with ΔN-Kcv mRNA were induced by voltage-steps from a holding potential (−20 mV) to test voltages as indicated. (*B*) Addition of 6 mM amantadine to the bath medium had only a minor effect on currents. (*C*) Steady-state I/V relations of currents recorded in the absence (●) and presence (○) of 6 mM amantadine in bath medium.

inhibitory effect of high positive and negative voltages on I_i was then estimated as a function of the ratio between the measured data points and the extrapolated linear current/voltage relation (I_{ex}/V). The voltage-dependence of the fractional decrease of I_i is shown in Fig. 4*B*. For a quantitative description of this plot the data from positive and negative voltages were fitted with the Boltzmann equation:

$$1 - (I_i/I_{ex}) = rB_{max}/(1 + \exp(zF(V_{0.5} - V)/RT)) \quad (1)$$

where rB_{max} denotes the maximal relative inhibition, z the voltage-sensitive coefficient and $V_{0.5}$ the voltage for half maximal inhibition. R, T and F have their usual thermodynamic meanings. Fitting data with Eq. 1 yielded for negative voltages the following parameters: maximal relative inhibition, $rB_{max} = 0.9$; voltage-dependent coefficient, $z_1 = -0.6$ and the voltage for half maximal inhibition, $V_{0.5,1} = -116$ mV. The corresponding values for positive voltages were: $rB_{max,2} = 0.6$; $z_2 = 1.9$; $V_{0.5,2} = +65$ mV. Results from fitting data from $n = 9$ oocytes are summarized in Table 1.

Time-dependent Component

To characterize the voltage-dependence of I_t, we determined the current-activation curve from the tail currents in Fig. 1*C*. The amplitude of the tail currents, measured immediately after stepping to −80 mV (Fig. 5*A*), were plotted against the conditioning voltage (−180 to +80 mV) after normalization. The resulting activation curve is shown in Fig. 5*B*. It was well fitted by a Boltzmann function yielding the coefficients $z_3 = 0.8$ and $V_{0.5,3} = -67$ mV. Results of fitting the data from $n = 7$ oocytes are summarized in Table 1.

We further characterized the kinetics of I_t activation and deactivation. For activation, steps were applied to test voltages between −40 mV and −160 mV from a holding voltage of +60 mV (Fig. 6*A*, top), at which voltage the time-dependent channels were closed (Fig. 5). For deactivation, the time-dependent component was fully activated at −160 mV and steps were applied in the range 0 mV to +60 mV (Fig. 6*A*, bottom). Both current activation and deactivation were best fitted by the sum of two exponentials (Fig. 6*A*). Plots of the voltage-dependence of the fast (τ_1) and slow (τ_2) time constants for activation and deactivation are shown in Fig. 6*B* and *C*, respectively. The data reveal a moderate voltage-dependence of τ_1 while τ_2 appears to be approximately voltage-independent.

While the time-dependent component reaches maximal activation at hyperpolarized voltages (Fig. 5*B*), the instantaneous component has maximal conductance at about 0 mV (Fig. 4*B*). Due to the opposite voltage-dependence of the two current components, it is not possible to obtain a "fully activated" I_{Kcv}. It is nevertheless possible to measure the "maximal" I_{Kcv} which includes a "fully activated" time-dependent component in addition to a steady-state instantaneous component. To measure the maximal I/V relation (I_{max}/V) for Kcv we used a three-step protocol, where the membrane was held at −20 mV and then stepped to a conditioning voltage of −160 mV for 1.5 sec to achieve full activation (Fig. 5*B*). From this conditioning voltage the membrane was stepped to test voltages between −100 mV and +80 mV. The amplitude of the currents measured immediately after stepping to the test voltages were plotted against the test voltages to yield the I_{max}/V relation shown in Fig. 7*A* (*filled circles*). For comparison also the steady-state I/V relation (I_{ss}/V), obtained as in Fig. 1, is plotted (*open circles*).

The I_{max}/V relation thus measured contains contributions from both the instantaneous and the fully-

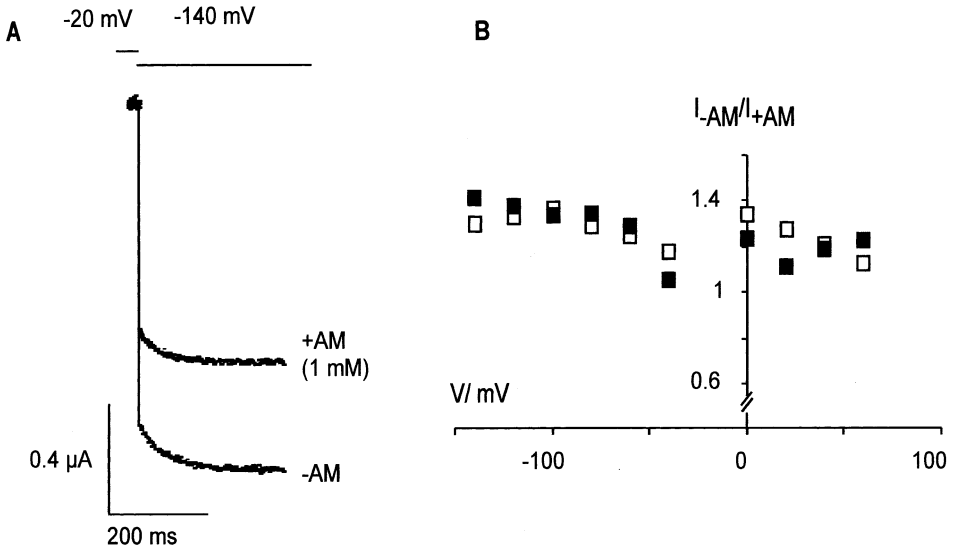

Fig. 3. Inhibition of instantaneous (I_i) and time-dependent (I_t) Kcv current by amantadine. (*A*) An oocyte expressing Kcv was clamped from −20 mV to −140 mV resulting in the typical instantaneous and time-dependent current response (*−AM*). Addition of 1 mM amantadine to the bath (*+AM*) caused a reduction of I_i and I_t. (B) Ratios of inhibition (I_{-AM}/I_{+AM}) for I_i (■) and I_t (□) over a range of test voltages. The plots show that both kinetic components are blocked in the same ratio.

activated time-dependent components. Since at $V > 40$ mV I_t is fully deactivated (Fig. 5), at positive voltages I_{ss} is composed of I_i only, while I_{max} now includes the contribution of the time-dependent component.

Fig. 7*B* shows that the ratio I_{ss}/I_{max} approaches at positive voltages a value of 0.7. This means that I_i contributes a fraction $a = 0.7$ and I_t, fraction $b = 0.3$ to the total current. In similar experiments with $n = 4$ oocytes we obtained mean values for a of 0.66 ± 0.02 and for b of 0.34 ± 0.02.

Formal Description of Kcv Current

With the above information it is possible to describe formally the Kcv current. The Kcv current $I(V,t)$ can be described as:

$$I(V,t) = g(V,t) \cdot (V - V_{K^+}), \tag{2}$$

where g is the conductance and V_{K^+} the equilibrium voltage for K^+.

The conductance $g(V,t)$ is given by the sum of the instantaneous (g_i) and the time-dependent (g_t) conductance:

$$g_i(V) = g_{max} \cdot \alpha \cdot a \tag{3}$$

$$g_t(V) = g_i \cdot \beta \cdot b \tag{4}$$

where g_{max} is the conductance of the maximal I/V relation (I_{max}/V); α is a factor that accounts for nonlinearity of the instantaneous current (relative inhibition) and can be derived from Fig. 4*B* as:

$$\alpha = 1 - rB_{max,1}/\{1 + \exp[z_1 F(V_{0.5,1} - V)/RT]\} - rB_{max,2}/\{1 + \exp[z_2 F(V_{0.5,2} - V)/RT]\} \tag{5}$$

The factor β describes the voltage-dependence of I_t. According to Fig. 5*B*

$$\beta = 1/\{1 + \exp[z_3 \cdot F(V_{0.5,3} - V)/RT]\}. \tag{6}$$

The factors a and b account for the fractional contribution of the instantaneous and time-dependent conductance, respectively, to $g(V,t)$. For the example of Fig. 1 they are estimated as $a = 0.7$ and $b = 0.3$ (Fig. 7).

$I(V,t)$ can be calculated from Eqs. 2–6 assigning values to $V_{0.5,x}$, Z_x, and $I_{max,x}$ from Figs. 4 and 5, values to a and b from Fig. 7, a g_{max} of 3×10^5 S (Fig. 7*A*) and a K^+ equilibrium voltage (V_{K^+}) of +10 mV. The calculated steady-state I/V relation is shown in Fig. 7*A* as a line. It is in good agreement with the corresponding measured steady-state I/V data (*open circles*), implying that Eqs. 2–6 are sufficient to describe the Kcv current. According to this description, about 70% of the channels are always open. At hyperpolarizing voltages the remaining 30% of the channels open in a voltage-dependent way.

The Mode of Voltage-Dependence

Voltage-dependence of voltage-dependent (Kv) channels is primarily determined by the movement of

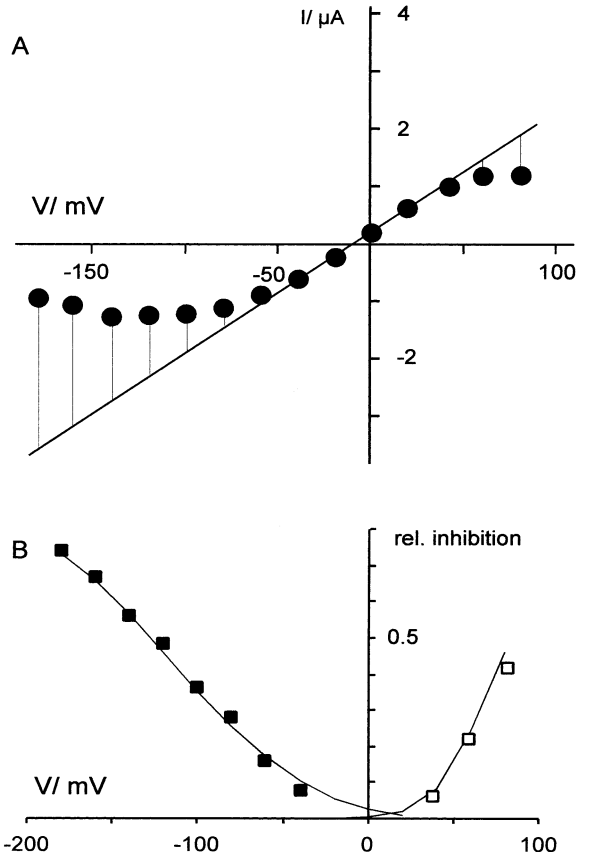

Fig. 4. Voltage-dependence of instantaneous Kcv current (I_i). (*A*) Voltage-dependent decrease of I_i (from Fig. 1) estimated as the difference between the measured I_i and the linear extrapolation of data points between −20 mV and +20 mV. (*B*) Relative inhibition (*rB*) plotted against voltage. Data for *rB* at negative (*filled squares*) and positive (*open squares*) voltages were jointly fitted (solid line) by Boltzmann functions (*see* text and Eq. 1) and yielded $rB_{max,1} = 0.9$; voltage-dependent coefficient, $z_1 = -0.6$ and voltage for half maximal inhibition, $V_{0.5,1} = -116$ mV for negative voltages. The corresponding values for positive voltages were: $rB_{max,2} = 0.6$; $z_2 = 1.9$; $V_{0.5,2} = +65$ mV.

the charged S4 segment in the membrane. In this context it was interesting to note that the short N-terminus of Kcv is slightly lipophilic and contains two charged amino acids, lysine (K5) and arginine (R10) (Plugge et al. 2000). Consequently we speculated that the N-terminus might be embedded in the membrane and serve as a cryptic voltage sensor. To test this hypothesis we mutated the two charged amino acids into neutral alanines. However, electrophysiological examination of the double mutant K5A R10A revealed no difference in the voltage-dependence of Kcv currents as compared to the wt-channel (*data not shown*).

Many K^+ channels are blocked by divalent cations in a voltage-dependent way (Hille, 1992). The Kcv channel is known to be blocked by external Ba^{2+} (Plugge et al. 2000). To test the possibility that a block by cations is responsible for the loss of linearity

Table 1. Parameters from fitting relative inhibition of instantaneous current (I_i) and activation curves of time-dependent current (I_t) to Boltzmann function

Parameter	I_i	I_t
z_1	−0.67 ± 0.08 (9)	
z_2	1.9 ± 0.11 (9)	
$V_{0.5,1}$	−113 ± 5 mV (9)	
$V_{0.5,2}$	85 ± 7 mV (9)	
rB_{max1}	0.92 ± 0.05 (9)	
rB_{max2}	0.61 ± 0.11 (9)	
z_3		−0.69 ± 0.04 (7)
$V_{0.5,3}$		−71 ± 6 mV (7)

Data obtained as in Fig. 4 for I_i and Fig. 5 for I_t. Values denote mean ± SD. Number of data sets in brackets. The parameters have the following meaning: *z*, voltage-sensitive coefficient; $V_{0.5}$, voltage for half maximal inhibition (I_i) or activation (I_t); rB_{max}, maximal relative inhibition.

of I_i at positive and negative potentials we changed the divalent cation concentration in the external medium. Fig. 8 shows that reducing Ca_o^{2+} had a strong effect on Kcv conductance. The sample current traces and the corresponding steady-state *I*/*V* relations reveal that lowering of Ca_o^{2+} over this moderate concentration range leads to an overall increase in both current components. In the present case a 10-fold reduction of Ca_o^{2+} caused a roughly 4-fold rise in Kcv current (Fig. 8*C*). In contrast, increasing Ca_o^{2+} relative to the control concentration reduced Kcv current (*data not shown*).

To examine whether the reduction of Kcv current by Ca_o^{2+} is voltage-dependent, we measured the ratio between the steady-state currents in 1.8 mM Ca_o^{2+} (reference level) and the currents in other Ca_o^{2+}. The plot shows that the effect of Ca_o^{2+} on I_{ss} is largely voltage-independent (Fig. 8*D*), a result confirmed in 3 other data sets.

The results in Fig. 8 indicate that Ca_o^{2+} affects Kcv current in a voltage-independent manner, suggesting that the current kinetics are Ca^{2+}-independent. To further investigate this point we examined the effects of Ca_o^{2+} on the kinetics of the time-dependent current component. We measured Kcv current during voltage steps from −20 mV to −160 mV in 1.8 and 0.18 mM Ca_o^{2+} and normalized the time-dependent current to the same amplitude. The traces superimpose almost perfectly, indicating that Ca_o^{2+} does not modify the current kinetics (Fig. 9). The same result was obtained for the kinetics of current deactivation at more positive voltages (Fig. 9).

For a quantification of the inhibitory effect of Ca_o^{2+} on the Kcv current, we plotted I_i recorded at −140 mV and +40 mV as a function of the external Ca^{2+} after normalization to the current in 1.8 mM Ca^{2+}. The graph shows a strong dependence of I_i on Ca^{2+} over a small range of concentrations. Inhibition already approaches saturation at Ca^{2+} con-

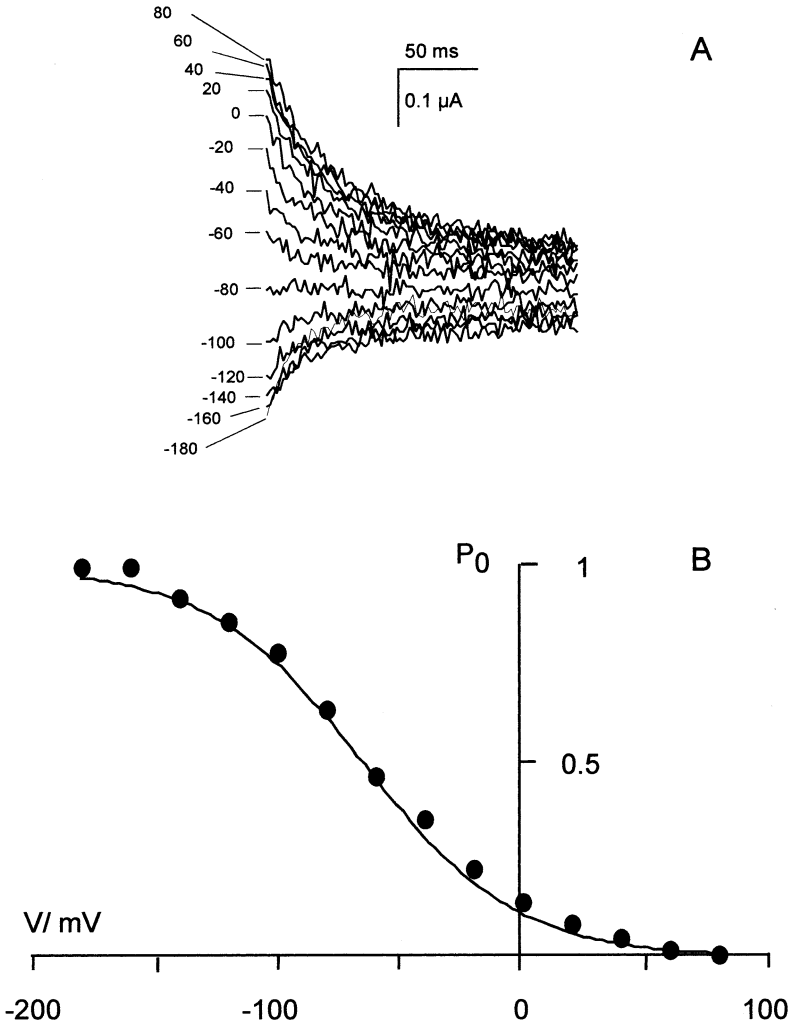

Fig. 5. Voltage-dependence of time-dependent (I_t) Kcv current. (*A*) Enlargement of tail currents from Fig. 1*C*. The currents were recorded at −80 mV following preconditioning at indicated voltages. (*B*) Normalized activation curve obtained from tail currents. Data were fitted with a Boltzmann function, such as Eq. 1, yielding $V_{0,5,3} = -67$ mV and $z_3 = 0.8$.

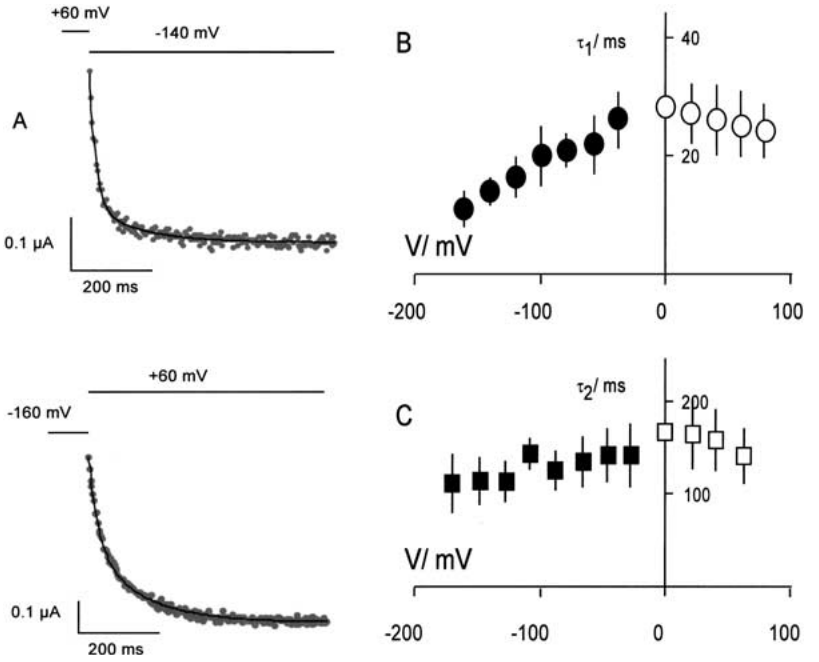

Fig. 6. Time constants for activation and deactivation of I_t as a function of voltage. An oocyte expressing Kcv was clamped to +60 mV to deactivate the time-dependent component. Steps to test voltages between −40 mV and −160 mV resulted in activation of I_t. Current activation kinetics was best described by the sum of two exponentials. Example of current response at −140 mV and fitting (*line*) is shown in *A* (*upper panel*). To follow deactivation the channels were first activated by clamping to −160 mV. Deactivation was monitored by stepping to test voltages between 0 and +60 mV. Deactivation kinetics was best described as the sum of two exponentials. Example of current response at +60 mV and fitting (*line*) is shown in *A* (*lower panel*). The mean fast (τ_1) and slow (τ_2) time constants for channel activation (*filled symbols*) and deactivation (*open symbols*) are plotted as a function of voltage in *B* and *C*, respectively.

centrations larger than about 2 mM (Fig. 10). However, full inhibition of Kcv current was not achieved by any Ca^{2+} concentration. Fitting with the Hill equation yielded a half-inhibition Ca_o^{2+} concentration of 0.34 mM and a Hill coefficient of 1.5.

In a previous study we had found that Kcv current is blocked in a strong voltage-dependent manner by Ba_o^{2+} (Plugge et al. 2000). The voltage-independent action of Ca^{2+} suggests the presence of an external binding site where cations interact with the channel protein. We then examined the specificity of it by analyzing the effect of Mg_o^{2+} on Kcv conductance. The stimulation of the Kcv current upon complete removal of Mg_o^{2+} was small. At -160 mV I_i increased on average by a factor of 1.2 ± 0.3, $n = 4$, for a tenfold reduction of Mg_o^{2+}.

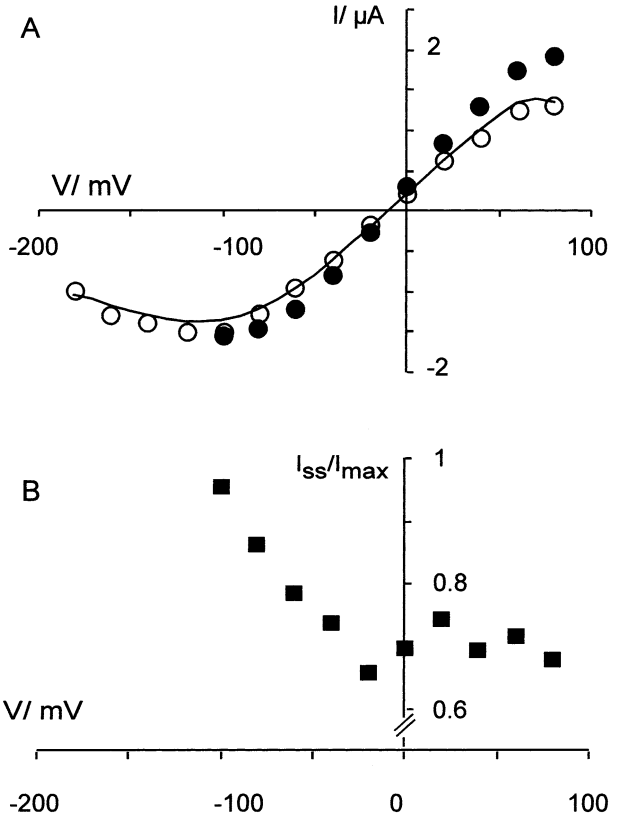

Fig. 7. Reconstruction of steady-state I/V relation from instantaneous and time-dependent components. (*A*) Maximal I/V relation of Kcv current. Data obtained from a two-step protocol, whereby the oocyte (same as in Fig. 1) was clamped to -160 mV to fully activate the time-dependent conductance. From the conditioning voltage the membrane was stepped to test voltages between -100 and 80 mV to collect the maximal current. The same procedure was repeated after inhibition of Kcv current with 6 mM amantadine. The I_{max}/V relation (●) plotted in *A* reports the steady-state values of the subtracted current. It has a maximal slope conductance of 29 µS. For comparison the corresponding steady-state I/V relation from Fig. 1 is also plotted (○). The smooth line represents the calculated steady-state I/V relation according to Eqs. 2–6 (*see* text) considering appropriate parameters from Figs. 4 and 5. (*B*) Ratio of steady-state and maximal currents from (*A*), I_{ss}/I_{max}, as a function of voltage.

Discussion

According to our data the conductance of the viral-encoded K^+ channel Kcv has a dual sensitivity to voltage. Considering the small size of the channel protein, this observation is important because this channel may contain the minimal structural requirements for voltage sensitivity of K^+ channels.

Analysis of the Kcv conductance shows a complex voltage-dependence. The conductance exhibits a maximum at about 0 mV. At this voltage the time-dependent fraction of channels (about 30% of the channels) is in a closed state, which they can leave upon hyperpolarization. Moving from zero mV towards hyperpolarizing or depolarizing voltages causes an instantaneous decrease in conductance. At hyperpolarizing voltages a slow increase of conductance (due to the opening of the time-dependent component) is superimposed on the rapid inhibiting process. It is worth noting that the amplitude of this time-dependent current undergoes the same inhibition as the instantaneous component. These results lead to the conclusions that Kcv has two antagonistic and overlapping voltage-sensitive mechanisms, one that opens channels at negative voltages and another one that inhibits conductance at both positive and negative voltages instantaneously.

The present data do not provide information about the mechanisms underlying the voltage-dependence nor about structural features of the channel protein involved in this process. Some of the mechanisms known to contribute to the voltage sensitivity of other K^+ channels can, however, be discarded. The responses of the channel conductance to changes in the extracellular cation concentration and composition indicate a cation-specific modulation of the Kcv channel conductance. However, changes in the extracellular concentration of Mg^{2+} or Ca^{2+} do not have any appreciable effects on the voltage sensitivity of either the instantaneous or the time-dependent component. These findings rule against the possibility that a voltage-dependent block of the Kcv channel by divalent cations is responsible for the decrease of the instantaneous conductance, at least at negative voltages.

In the family of Kv channels, charged amino acids located in the S4 segment serve as the dominant voltage sensor (Bezanilla, 2000). Kcv lacks an S4 segment, but the short N-terminus of the protein contains 2 positively charged aa in a hydrophobic region that may be located in the membrane. However, Kcv voltage sensitivity was unchanged when the two charged aa were replaced with alanines. This finding indicates that these charged aa do not con-

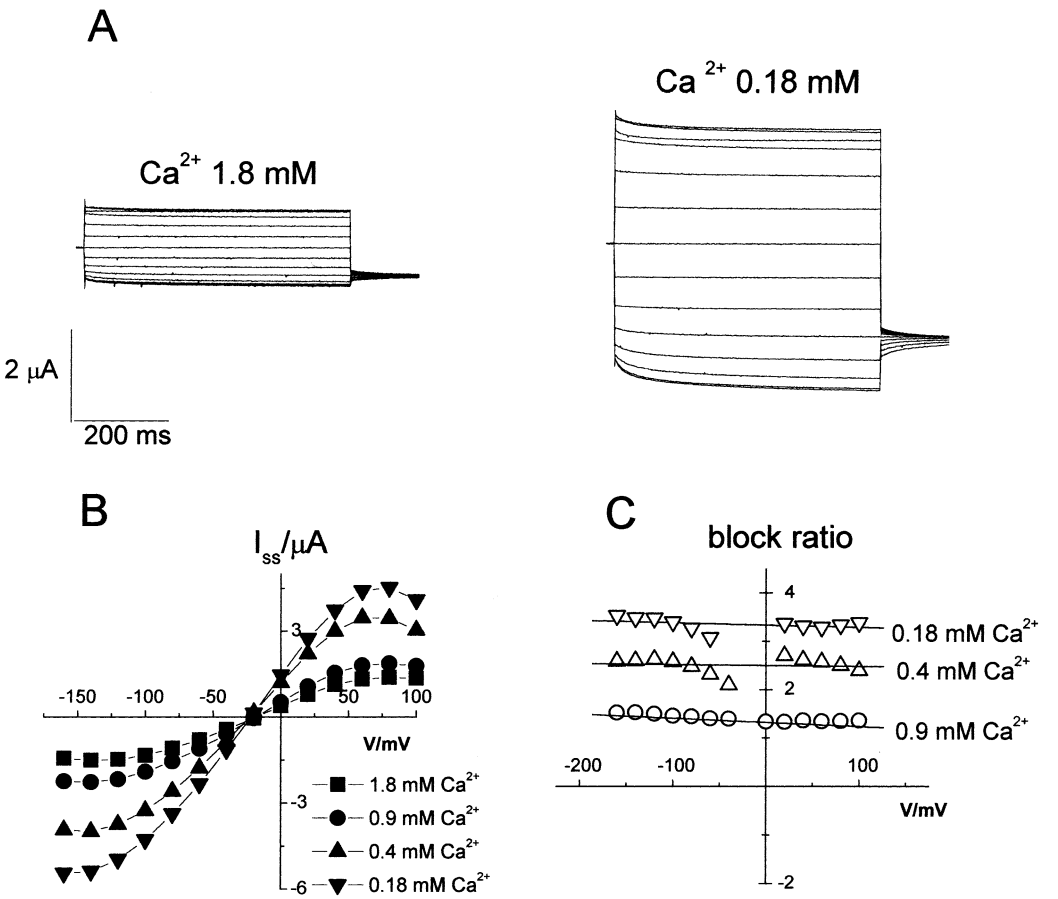

Fig. 8. Lowering of Ca_o^{2+} increases Kcv current. (*A*) Current responses to voltage steps from −20 mV to test voltages between +100 mV and −160 mV in an oocyte expressing Kcv in the presence of 1.8 mM or 0.18 mM Ca_o^{2+}. (*B*) Steady-state *I*/*V* relation from the same oocyte measured at the indicated calcium concentrations. (*C*) Voltage-independence of the effect of calcium. Ratios of the current measured in 0.18 mM Ca_o^{2+} (reference concentration) and those of other Ca_o^{2+}.

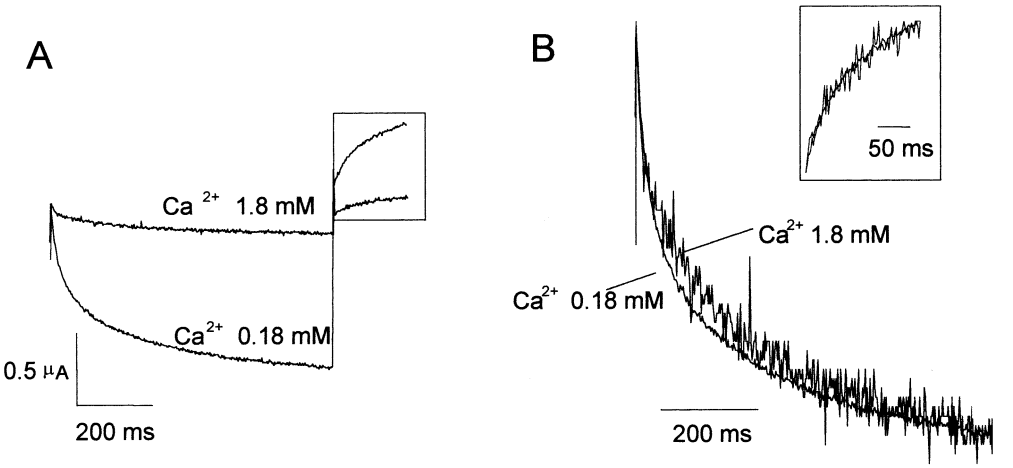

Fig. 9. Activation and deactivation kinetics of I_t in different $[Ca^{2+}]_o$. (*A*) Time-dependent components of current responses to voltage steps from −20 mV to −160 mV and return to −80 mV in low and high external calcium. Current activation kinetics (at −160 mV) (*B*) and deactivation kinetics (at −80 mV) (*Inset*) recorded in both Ca_o^{2+} normalized to the same ordinate.

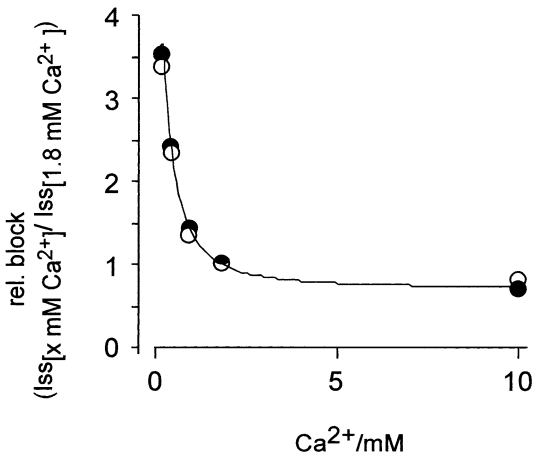

Fig. 10. Relative inhibition of I_{ss} as a function of Ca_o^{2+}. I_{ss} recorded at −140 mV (*filled symbol*) and +40 mV (*open symbol*) normalized to respective reference I_{ss} at these voltages in 1.8 mM Ca_o^{2+} plotted as a function of the external Ca_o^{2+}. The smooth curve was obtained by fitting data with Hill equation $y = I_m\{1 - 1/[1 + (k_{0.5}/Ca_o^{2+})]^n\}$ were I_m is th relative asymptotic current at low Ca_o^{2+} (3.57 relative units), $k_{0.5}$ (0.34 mM) is Ca_o^{2+} producing half-maximal inhibition, and n (1.5) is the Hill coefficient. Mean data from 3 to 8 experiments.

tribute to the voltage sensor. The only remaining candidates for voltage sensing are one charged aa in the first transmembrane segment and several charged aa in the pore loop, whose relevance remains to be investigated.

Whereas the nonlinearity of the Kcv I/V relation is unmodified by extracellular calcium, its conductance is nevertheless very sensitive to extracellular calcium concentration; our data suggest that the channel possesses a binding site at the outer pore mouth, which discriminates between divalent cations. Occupation of this site by Ca^{2+} reduces the channel conductance over the entire voltage spectrum. A possible explanation for this finding is that Ca^{2+} reduces the unitary channel conductance. As in native K^+ channels, Ca^{2+} might also cause a voltage-independent flicker-block of the open Kcv channel (Shioya, Matsuda & Noma, 1993; Vassilev et al. 1997).

Conclusions

Central to the voltage sensitivity of various ion channels are structural elements in the channel protein. These elements either cause a voltage-dependent conformational change in the protein (as in the Kv channel family, Bezanilla, 2000) or interact specifically with blocking ions (as in the Kir channel family, Lopatin, Makina & Nichols, 1994; Lu & MacKinnon, 1994). The viral-encoded Kcv K^+-channel is structurally simpler than either the Kv or Kir channel. The Kcv protein has two TM domains, and its cytoplasmic N- and C-termini are either very short (N-terminus, 12 aa) or absent (C-terminus). Consequently, Kcv lacks most of the structural elements such as the V-sensor, or the T1-domain (Cushman et al., 2000), which are contributing to the voltage sensitivity of K^+ channels. The results presented in this work indicate that despite its structural simplicity, Kcv has two mechanisms that are independently sensitive to voltage.

We thank J. Dainty (Norwich) for help with the manuscript. AM and GT were supported by the bi-national traveling grant *Vigoni*. AM was supported by Ministero delle Politiche Agricole e Forestalli, Piano Nazionale Biotecnologie.

References

Bezanilla, F. 2000. The voltage sensor in voltage-dependent ion channels. *Physiol. Rev.* **80:**555–592

Clapham, D.E. 1999. Unlocking family secrets: K^+ channel transmembrane domains. *Cell* **97:**547–550

Cushman, S.J., Nanao, M.H., Jahng, A.W., DrRubeis, D., Choe, S., Pfaffinger, P.J. 2000. Voltage dependent activation of potassium channels is coupled to T1 domain structure. *Nature Struct. Biol.* **7:**403–407

Doupnik, C.A., Davidson, N., Lester, H.A. 1995. The inward rectifier potassium channel family. *Curr. Opin. Neurobiol.* **5:**268–277

Doyle, D.A., Cabral, J.M., Pfuetzner, R.A., Kuo, A., Gulbis, J.M., Cohen, S.L., Chait, B.T., MacKinnon, R. 1998. The structure of the potassium channel: molecular basis of K^+ conduction and selectivity. *Science* **280:**69–77

Hille, B. 1992. Ionic channels of excitable membrances. Sinauer Associates, Sunderland, MA

Lopatin, A.N., Makina, E.N., Nichols, C.G. 1994. Potassium channel block by cytoplasmic polyamines as the mechanism of intrinsic rectification. *Nature* **24:**372–366

Lu, Z., MacKinnon, R. 1994. Electrostatic tuning of Mg^{2+} affinity in an inward-rectifier K^{2+} channel. *Nature* **371:**243–246

Moroni, A., Barbuti, A., Altomare, C., Baruscotti, M., DiFrancesco, D. 2000. Kinetic and ionic properties of the human HCN2 pacemaker channel. *Pfluegers Arch. Eur. J. Physiol.* **439:**618–626

Moroni, A., Bardella, L., Thiel, G. 1998. The impermeable ion methylammonium blocks K^+ and NH_4^+ currents through KAT1 channels differently: evidence for ion interaction in channel permeation. *J. Membrane Biol.* **163:**25–35

Perozo, E., Cortes, D.M., Cuello, L.G. 1998. Three-dimensional architecture and gating mechanism of a K^+ channel studied by EPR spectroscopy. *Nature Struct. Biol.* **5:**459–469

Plugge, B., Gazzarrini S., Nelson M., Cerana R., Van Etten J.L., Derst C., DiFrancesco D., Moroni A., Thiel G. 2000. A new potassium channel protein encoded by chlorella virus PBCV-1. *Science* **287:**1641–1644

Shioya, T., Matsuda, H., Noma, A. 1993. Fast and slow blockades of the inward-rectifier K^+ channel by external cations in guinea-pig cardiac myocytes. *Pfluegers Arch.* **422:**427–435

Schrempf, H., Schmidt, O., Kummerlen, R., Hinnah, S., Muller.D., Betzler, M., Steinkamp, T., Wagner, R. 1995. A proharyotic

potassium ion channel with two predicted transmembrane segments from *Streptomyces lividans*. *EMBO J*. **14:**5170–5178

Van Etten, J.L., Meints R.H. 1999. Giant viruses infecting algae. *Ann. Rev. Microbiology* **53:**447–494

Vassiliev, P.M., Kanazirska, P.V., Ye, C., Francis, J., Hong, K., Brown, E.M. 1997. A flickery block of a K^+ channel mediated by extracellular Ca^{2+} and other agonists of the Ca^{2+} sensing receptors in dispersed bovine parathyroid cells. *Biochem. Biophys. Res. Comm*. **230:**616–623

Wei, A., Jegla, T., Salkoff, L. 1996. Eight potassium channel families revealed by the *C. elegans* genome project. *Neuropharm*. **37:**805–829